www.czasopisma.pan.pl PAN POLSKA AKADEMIA NAUK www.journals.pan.pl

Arch. Metall. Mater. **64** (2019), 3, 851-855

DOI: 10.24425/amm.2019.129460

MIN-JIN LEE*, HYUN-AH JUNG*, KYONG-JIN LEE*, HAEJIN HWANG*#

FABRICATION OF AGAR-SILICA AEROGEL NANOCOMPOSITE FILMS

In this study, agar-based nanocomposite films containing ultra-porous silica aerogel particles were fabricated by gel casting using an aqueous agar/silica aerogel slurry. The silica aerogel particles did not show significant agglomeration and were homogeneously distributed in the agar matrix. Transmission electron microscopy observations demonstrated that the silica aerogel particles had a mesoporous microstructure and their pores were not incorporated into the agar polymer molecules. The thermal conductivities of the agar and agar/5 wt.% silica aerogel nanocomposite films were 0.36 and 0.20 $W \cdot m^{-1} \cdot K^{-1}$, respectively. The transmittance of the agar films did not decrease upon the addition of silica aerogel particles into them. This can be attributed to the anti-reflection effect of silica aerogel particles.

Keywords: thermal insulation film, silica aerogel, agar, thermal conductivity, transmittance

1. Introduction

Thermal insulation of buildings and houses requires a large amount of energy to maintain an optimum temperature and humidity using air conditioners and is a major concern from the environmental viewpoint. This is because it accounts to about 30% of the global carbon dioxide (CO_2) emission. Over the past few years, buildings with all-glass curtain walls have been constructed extensively. In winter, the heat loss through glass walls or windows is much greater than that through concrete walls. In summer, the radiant heat induces glass greenhouse effect. Hence, it is imperative to develop a high-performance daylight insulation system [1].

Silica aerogels are made up of highly cross-linked networks of silica nanoparticles and exhibit unusual properties such as ultra-high porosity (>95%), high specific surface area (500-1000 $m^2 \cdot g^{-1}$), low thermal conductivity (20-30 $mW \cdot m^{-1} \cdot K^{-1}$), low relative permittivity (1-2), and low index of refraction (~1) [2]. Owing to these unique properties, silica aerogels have gained immense attention as catalysts and thermal insulators and in applications related to adsorption and drug delivery. The extremely low thermal conductivity of these aerogels makes them potential material for energy-efficient buildings and houses [3,4].

However, silica aerogel monoliths or boards suffer from low flexibility, strength, and reproducibility, which limit their application as a building material [5]. Although efforts have been made to fabricate composite-type silica aerogels and to enhance their thermal and mechanical properties, reducing the complexity of the synthesis processes and inhomogeneity of the composite composition remains challenging [6,7].

Agar is a natural polymer, which is derived from red algae such as agarophytes, and its structure is characterized by a heterogeneous mixture of two polysaccharides: agaropectin, a charged/sulfated polymer, and agarose, a neutral polymer [8]. Agar dissolves in hot water and sets to a rigid gel at 32-45°C. The strength of agar gels depends on the concentration, time, pH, and sugar content [9,10]. In this study, agar-silica aerogel nanocomposite films were fabricated using agar and a silica aerogel powder by a very simple fabrication method. The effect of the silica aerogel content on the microstructure and thermal performance of the resulting agar/silica aerogel nanocomposite films was investigated.

2. Experimental

Agar (1.8 g, Extra pure grade, Ducksan, Korea) and glycerol (1.8 g, ≥99.0%, Sigma-Aldrich, as a plasticizer) were dissolved in 50 g of hot water. Silica aerogel powder (Enova mt1100, Cabot Corp.) was dispersed in 30 mL of ethyl alcohol (99.5%, Samchun Pure Chemical, Korea). Span 80 ($C_{24}H_{44}O_6$, Junsei, Japan) was then added to the resulting silica aerogel slurry in order to enhance its stability. Then, the agar solution and silica aerogel slurry were mixed under stirring and the resulting viscous slurry was cooled down to 30°C. This slurry was then poured on a petri dish to make a gel film. The weight fraction of the silica aerogel powder was 1, 2, 3, 4, and 5 with respect to agar and glycerol.

* INHA UNIVERSITY, DEPARTMENT OF MATERIALS SCIENCE AND ENGINEERING, 100 INHA-RO, NAM-GU INCHEON 22212, KOREA

Corresponding author:hjhwang@inha.ac.kr

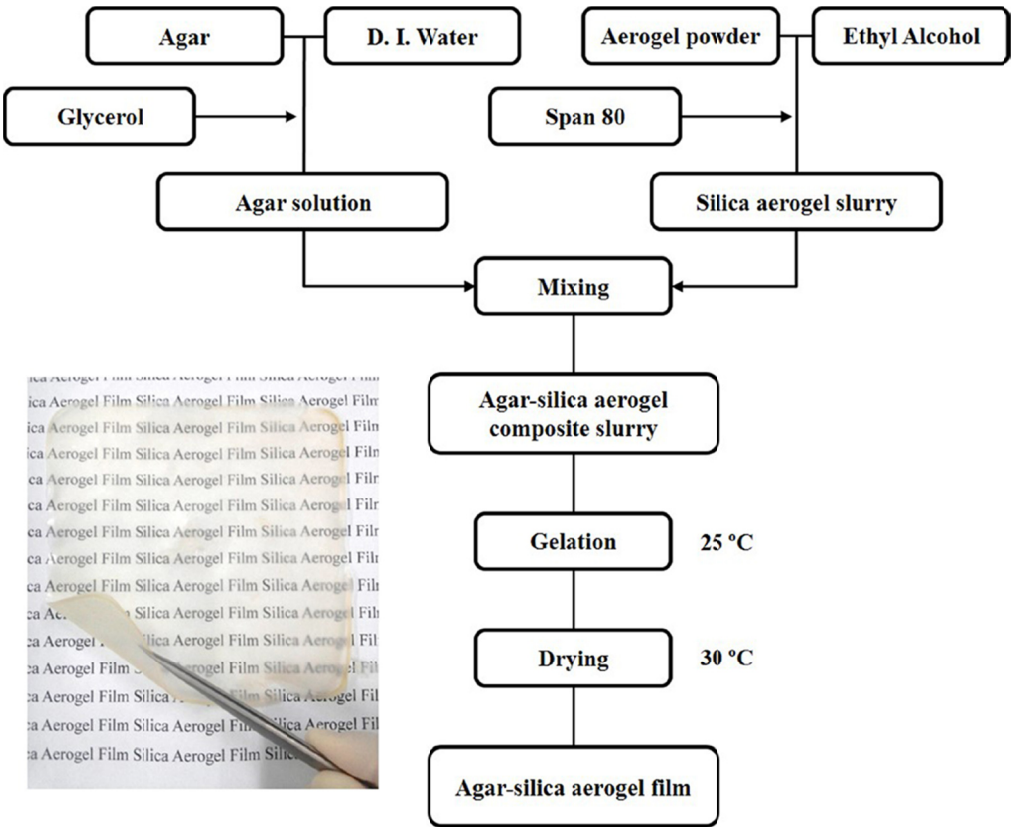

Fig. 1. Experimental flow chart for the fabrication of the agar/silica aerogel nanocomposite films

The gel film was maintained at 30°C for 24 h. Fig. 1 illustrates the fabrication process for the agar-silica aerogel nanocomposite film. As can be seen from its photograph (Fig. 1), the agar film was flexible and translucent.

The surface structure of the agar-silica aerogel nanocomposite films was examined by a field emission scanning electron microscope (FE-SEM, S-3200, Philips). Energy dispersive X-ray spectroscopy (EDS) was used to confirm the dispersion of silica aerogel particles in the films. The pore structure of silica aerogel was investigated using transmission electron microscope (TEM). For TEM analysis, the agar-silica aerogel films were frozen in liquid nitrogen and cut into 0.1-mm thick slices.

The thermal conductivity (κ) of the films was determined from their thermal diffusivity, α, using the laser flash method (Netzsch Instrument, Inc., Burlington, USA), and the specific heat capacity, c_p, was measured by differential scanning calorimetry. The thermal conductivity of the films was calculated using the equation: $\kappa = \alpha \rho c_p$, where ρ is the density of the films. The transmittance of the films was measured using a double-beam ultraviolet/visible/near infrared (UV/VIS/NIR) spectrometer (Carry 100 Bio, Varian).

3. Results and discussion

Figs. 2(a) and (b) show the cross-sectional SEM images of the agar and agar/5 wt.% silica aerogel nanocomposite films, respectively. The side surfaces of the agar film were very smooth

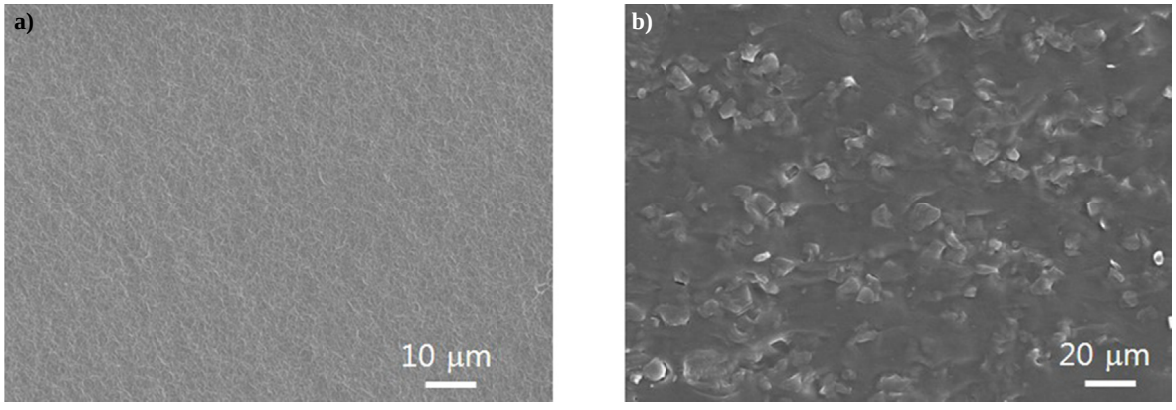

Fig. 2. SEM images of the agar (a) and agar/5wt% silica aerogel nanocomposite (b) films

(Figs. 1 and 2(a)). Fig. 2(b) shows that silica aerogel particles were uniformly distributed in the composite film. The particle size of the composite film was estimated to be ~5-10 μm, which was nearly the same as that of the silica aerogel precursor. This suggests that silica aerogel particles did not agglomerate during the film fabrication processes such as mixing and drying.

The agar/silica aerogel nanocomposite film was characterized by carrying out SEM and EDS analyses. Fig. 3(a) shows the surface SEM image of the agar/5 wt.% silica aerogel nanocomposite film. Figs. 3(b) and (c) show the EDS elemental mapping of silicon and oxygen, respectively for the composite film. The EDS analysis showed that SiO_2 particles were dispersed in the nanocomposite film. This confirmed the presence of silica aerogel in the film. In addition, Figs. 1 and 2 clearly show that silica aerogel particles were homogeneously distributed in the agar matrix.

Agar shows hydrophilic characteristics, while silica aerogel particles show hydrophobic characteristics because their surface is chemically modified by the hydrophobic CH_3 functional groups [11]. This difference in the surface characteristics of silica aerogel particles and agar make it difficult to disperse silica aerogel particles in aqueous agar/glycerol solutions. In our previous study on the stability of silica aerogel slurries, it was found that silica aerogel particles are stable in ethanol/water solutions [12]. In this study, as mentioned in the experimental section, silica aerogel powder was dispersed in ethyl alcohol, in which silica aerogel particles do not form a stable slurry. However, when the slurry was added to an aqueous solution of agar/glycerol, the silica aerogel particles maintained their stability in the slurry for prolonged times. In the ethyl alcohol/water solution, the pores of the silica aerogel particles were preferentially filled with ethyl alcohol, while water was expelled from the silica aerogel particles, resulting in the formation of a stable slurry. The formation of this stable slurry resulted in a homogeneous distribution of silica aerogel particles in the agar film, as shown by Figs. 1 and 2.

There are two important factors that should be considered while fabricating silica aerogel/polymer nanocomposites: 1) uniform dispersion of silica aerogel particles in the polymer matrix and 2) the pore structure of silica aerogel. In particular, the polymer or binder should not be incorporated into the silica aerogel pore structure [13]. If the pores of silica aerogel are filled with polymer molecules, then the resulting composites do not show the advantages of blending the silica aerogel, for example, low density and low thermal conductivity [14]. Fig. 4 shows the TEM images and EDS elemental analysis result of the agar/5 wt.% silica aerogel nanocomposite film. The TEM images revealed that the film showed a mesoporous microstructure that is typically observed in silica aerogels [15]. As is evident from Fig. 4 (the right TEM image), agar molecules were not incorporated into the pores of silica aerogel. The pore diameter was estimated to be ~10-20 nm. The EDS analysis confirmed that silica particles were present in the composites.

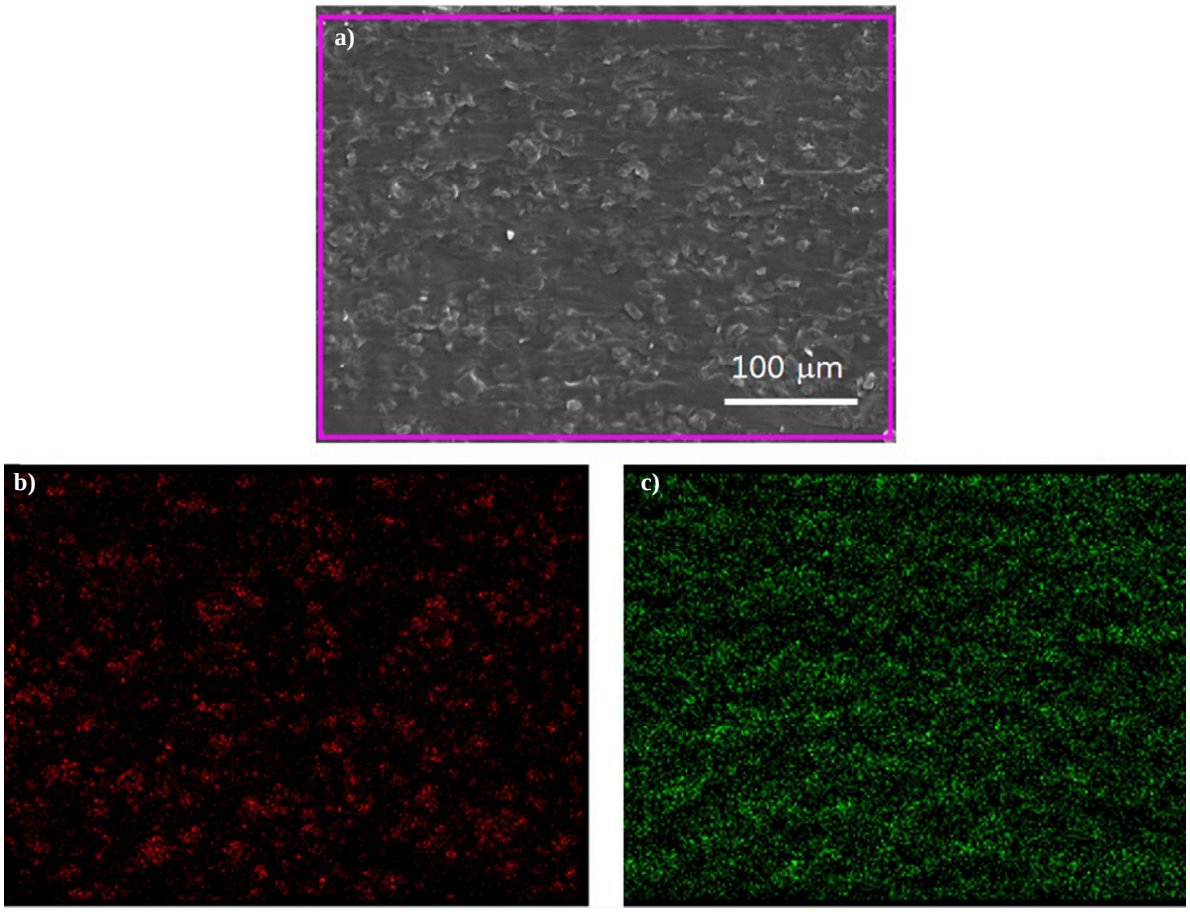

Fig. 3. SEM image (a) and the corresponding EDS mapping of silicon (b) and oxygen (c) for the agar/5wt% silica aerogel nanocomposite film

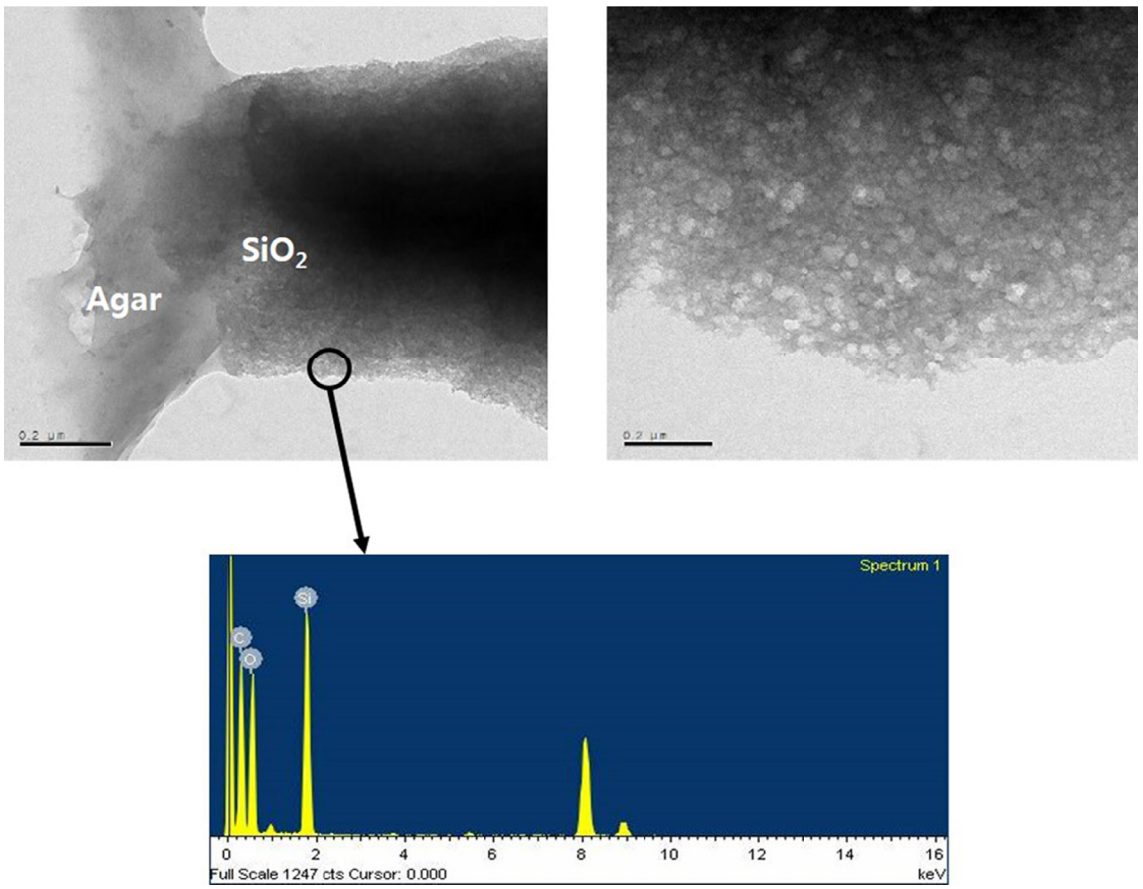

Fig. 4. TEM images and EDS elemental analysis result of the agar/5wt% silica aerogel nanocomposite film

The thermal conductivity of silica aerogel is extremely low because heat transfer occurs mainly through its pores [11,16]. Fig. 5 shows the thermal conductivities of the agar and silica aerogel nanocomposite films as a function of the silica aerogel content. The thermal conductivity of the agar film was 0.36 $W \cdot m^{-1} \cdot K^{-1}$ and it gradually decreased with an increase in the silica aerogel content. This result is somewhat reasonable since the thermal conductivity of silica aerogel is much lower than that of agar.

Interestingly, the thermal conductivity of the agar/silica aerogel nanocomposite film decreased further (as low as 0.10 $W \cdot m^{-1} \cdot K^{-1}$, which is one third of the thermal conductivity of the agar film) when large silica aerogel particles were incorporated into the agar matrix. Only the silica aerogel pores that were not filled with agar contributed to the thermal conductivity reduction. With an increase in the size of the silica aerogel particles, the volume of the pores that did not contain agar increased.

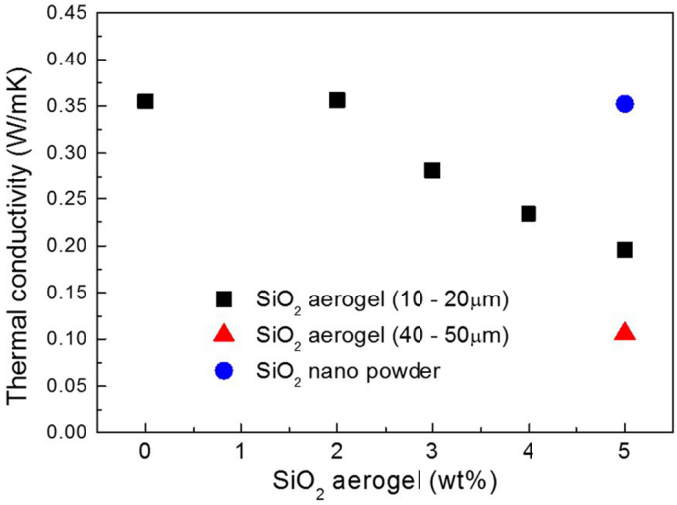

Fig. 5. Thermal conductivity of the agar and agar/silica aerogel nanocomposite films

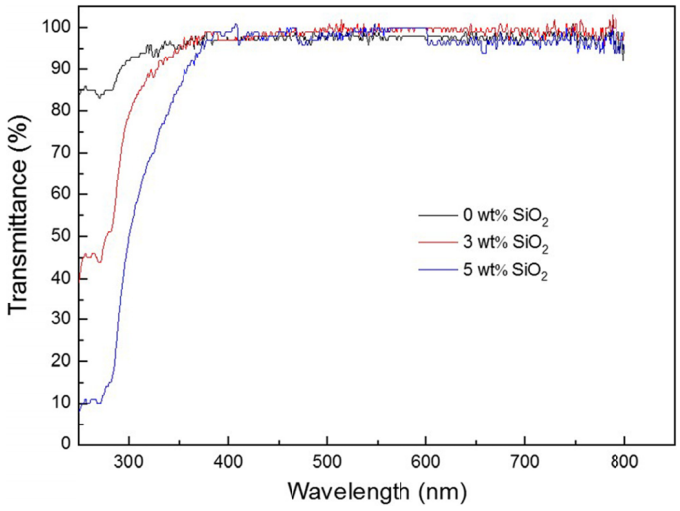

Fig. 6. Transmittance of the agar and agar/silica aerogel nanocomposite films. The films with 0, 3, and 5 wt.% silica had a thickness of 0.17, 0.20, and 0.23 mm, respectively

Fig. 6 shows the optical transmittance spectra of the agar and silica aerogel nanocomposite films in the UV-VIS-NIR region. Both the agar and silica aerogel nanocomposite films showed good visible and near infrared light transmittance of ~95%. This indicates that silica aerogel did not reduce the transmittance of the agar film. The silica aerogel particles used in this study were relatively large (10-20 μm) and thus could scatter the incident visible or infrared lights, leading to a reduction in the transmittance. In addition, silica aerogel shows an anti-reflective property [17]. Therefore, the transmittance reduction owing to the scattering by silica aerogel particles was counteracted by their reduced surface reflection. The strong absorption in the ultraviolet region can be ascribed to the presence of silica aerogel particles [18]. The absorption increased with an increase in the silica aerogel content.

4. Conclusions

An agar-based nanocomposite films containing ultra-porous silica aerogel particles were fabricated by gel casting using an aqueous agar/silica aerogel slurry. The silica aerogel particles did not show significant agglomeration and were homogeneously distributed in the agar matrix. Transmission electron microscopy observations demonstrated that the silica aerogel particles dispersed in the agar matrix exhibited a mesoporous microstructure, indicating that agar polymer was not incorporated into the pores of silica aerogel during the fabrication of the films. And the thermal conductivity of the agar film decreased with an increase in the silica aerogel content. The thermal conductivity of the agar/5 wt.% silica aerogel nanocomposite film was lower ($0.20\ W \cdot m^{-1} \cdot K^{-1}$) than that of the agar film ($0.36\ W \cdot m^{-1} \cdot K^{-1}$). Besides the transmittance of the agar films did not decrease upon the addition of silica aerogel particles into them. This can be attributed to the anti-reflection effect of silica aerogel particles.

Acknowledgments

This study was supported by an Inha University Research Grant. This work was also supported by the Korea Institute of Energy Technology Evaluation and Planning(KETEP) and the Ministry of Trade, Industry & Energy(MOTIE) of the Republic of Korea (No. 20194030202340).

REFERENCES

[1] R. Baetens, B.P. Jelle, A. Gustavsen, Energy and Buildings **43**, 761-769 (2011).
[2] V.G. Parale, K.Y. Lee, H.H. Park, J. Korean Ceram. Soc. **54**, 184-199 (2017).
[3] M. Reim, W. Körner, J. Manara, S. Korder, M. Arduini-Schuster, H.P. Ebert, J. Fricke, Solar Energy **79**, 131-138 (2005).
[4] Y. Huang, J.lei. Niu, Energy **83**, 316-325 (2015).
[5] J.C.H. Wong, H. Kaymak, P. Tingaut, S. Brunner, M.M. Koebel, Microporous and Mesoporous Mater. **217**, 150-158 (2015).
[6] A. Fidalgo, J.P.S. Farinha, J.M.G. Martinho, M.E. Rosa, L.M. Ilharco, Chem. Mater. **19**, 2603-2609 (2007).
[7] H. Maleki, L. Durães, A. Portugal, J. Non-Crystalline Solid **385**, 55-74 (2014).
[8] C.H. Lee, E.J. Yun, H.T. Kim, I.G. Choi, K.H. Kim, Process Biochem. **50**, 1629-1633 (2015).
[9] M. Lahaye, C. Rochas, Hydrobiologia **221**, 137–148 (1991).
[10] M. Zhang, Z. Che, J. Chen, H. Zhao, L. Yang, Z. Zhong, J. Lu, J. Chem. Eng. Data **56**, 859-864 (2011).
[11] K.J. Lee, Y.H. Kim, J.K. Lee, H. Hwang, Chemistry Select **3**, 1257-1261 (2018).
[12] K.J. Lee, Y.J. Choe, Y.H. Kim, J.K. Lee, H. Hwang, Ceram. Inter. **44**, 2204-2208 (2018).
[13] S.Y. Kim, Y.J. Noh, J. Lim, N. You, Macromolecular Research **22**, 108-111 (2014).
[14] H. Chen, V.V. Ginzburg, J. Yang, Y. Yang, W. Liu, Y. Huang, L. Du, B. Chen, Progress in Polymer Sci. **59**, 14-85 (2016).
[15] L. Brigo, E. Scomparin, M. Galuppo, G. Capurso, M.G. Ferlin, V. Bello, N. Realdon, G. Brusatin, M. Morpurgo, Mater. Sci. Eng.: C **59**, 585-593 (2016).
[16] S.K. Seo, J.W. Park, H.K. Cho, Y.S. Chu, J. Korean Ceram. Soc. **55**, 61-66 (2018).
[17] G.S. Kim, S.-H. Hyun, J. Non-Crystalline Solids **320**, 125-132 (2003).
[18] J.S. Lee, S.-C. Moon, K.-J. Noh, S.-E. Lee, J. Korean Ceram. Soc. **54**, 429-437 (2017).